Multiple Heads are Better than One: Few-shot Font Generation with Multiple Localized Experts - Appendix -

Appendix

We describe additional experimental results to complement the main paper (§A). The implementation details are in §B. Finally, we provide the detailed evaluation protocols (§C).

A. Additional experimental results

A.1. More visual examples

We show more generated glyphs in Figure A.2. MX-Font correctly synthesizes the strokes, dot, thickness and size of the ground truth glyphs. In the cross-lingual FFG, MX-Font can produce promising results in that they are all readable. Meanwhile, all other competitors provide inconsistent results, which are often impossible to understand. These results show a similar conclusion as our main paper.

A.2. Impact of the number of experts

In Table A.1, we report the performances by varying the number of experts, k. We observe that larger k brings better performances until $k = 6$, but larger k, *e.g.*, 8, shows slightly worse performance than $k = 6$. We presume that this is because there are no sufficient data having more than or equal to eight components for training all the eight experts to capture different concepts. Figure A.1 illustrates the frequency of the number of components. From this graph, we find that the most characters have less than 8 components in our Chinese dataset. Moreover, larger k means the number of parameters are increased, resulting in more training and inference runtime. Hence, in the paper, we choose $k = 6$ for all experiments.

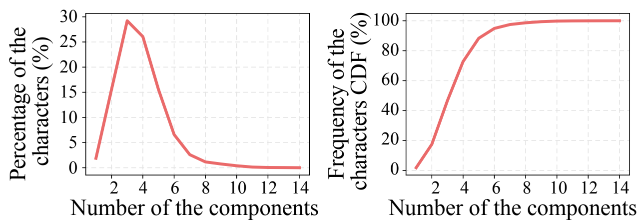

Figure A.1. **The distribution of number of components.** The left shows the percentage of characters with different number of components and the right shows the cumulative summation of the left.

k	Acc (S) ↑	Acc (C) ↑	Acc (B) ↑	LPIPS ↓
1	72.2	98.7	71.4	0.133
2	79.0	99.3	78.5	0.128
4	78.3	99.5	78.0	0.125
6	78.9	**99.5**	**78.7**	**0.120**
8	75.5	99.5	75.2	0.123

Table A.1. **Impact of the number of experts k.** The models with different number of heads are compared on in-domain Chinese transfer benchmark. We used $k = 6$ for all experiments.

B. Implementation details

B.1. Network architecture

Each localized expert E_i has 11 layers including convolution, residual, global-context [3], and convolutional block attention (CBAM) [18] blocks. The multiple localized experts share the weights of their first five blocks. The two feature classifiers Cls_s and Cls_u have the same structure; a linear block following two residual blocks. The weights of the first two residual blocks are shared. The generator G consists of convolution and residual blocks. Please refer our code for the detailed architecture.

B.2. Component allocation problem to weighted bipartite B-matching problem

Given a bipartite graph $G = (V, E)$, where V is a set of vertices, E is a set of edges and W is the weight values for each edge $e \in E$, the weighted bipartite B-matching (WBM) problem [13] aims to find subgraph $H = (V, E')$ maximizing $\sum_{e \in E} W(e)$ with every vertex $v \in V$ adjacent to at most the given budget, $B(v)$, edges. WBM problem can be solved by the Hungarian algorithm [14], a typical algorithm to solve combinatorial optimization in a polynomial time, in $O(|V||E|) = O(|V|^3)$. For curious readers, we refer recent papers solving variants of WBM problems [5, 1].

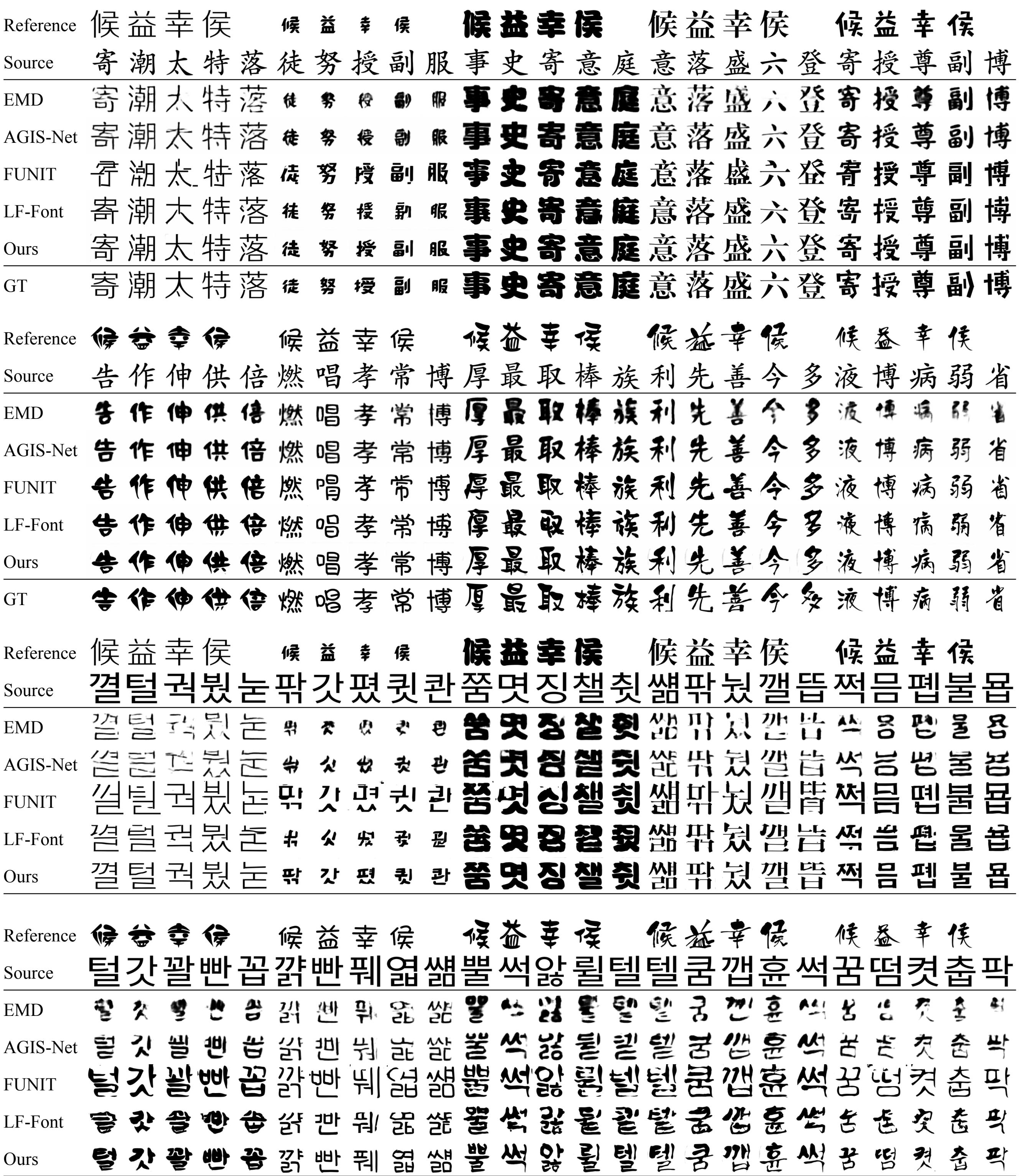

Figure A.2. **Generation samples.** We provide more generated glyphs with four reference glyphs.

We recall the component allocation problem described in the main paper:

$$
\begin{aligned}
&\max_{w_{ij}\in\{0,1\}|i=1\dots k, j\in U_c} \sum_{i=1}^{k}\sum_{j\in U_c} w_{ij}p_{ij},\\
\text{s.t.}\quad & \sum_{i=1}^{k} w_{ij} \geq 1 \ \text{ for } \forall j, \quad \sum_{j\in U_c} w_{ij}\geq 1 \ \text{ for } \forall i,\\
& \sum_{j\in U_c} w_{ij} \leq \max\left(1, \left\lceil \frac{m}{k} \right\rceil\right) \ \text{ for } \forall i\\
& \sum_{i=1}^{k} w_{ij} \leq \max\left(1, \left\lceil \frac{k}{m} \right\rceil\right) \ \text{ for } \forall j.
\end{aligned} \tag{B.1}
$$

We replace the last condition, $\sum_{i=1}^{k}\sum_{j\in U_c} w_{ij} = \max(k,m)$ to the upper bound condition where $\lceil\cdot\rceil$ denotes the ceiling function. For example, if $k=3$ and $m=4$, the budget for each expert is 2, while the budget for each component is 1. We build a bipartite graph where the vertex set contains all experts and all valid components, and the edge weights are the prediction probability p_{ij}. Now (B.1) can be re-formulated by the WBM problem.

B.3. HSIC Formulation

When training MX-Font, we let the two feature outputs from different experts, or content and style features independent of each other. To measure the independence between content feature and style feature, we first assume that the content features f_c and the style features f_s are drawn from two different random variables, Z_c and Z_s, *i.e.*, $f_c \sim Z_c$ and $f_s \sim Z_s$. We employ Hilbert Schmidt independence criterion (HSIC) [7] to measure the independence between two random variables. For two random variables Z_c and Z_s, HSIC is defined as $\text{HSIC}^{k,l}(Z_c,Z_s) := ||C^{k,l}_{Z_cZ_s}||^2_{\text{HS}}$ where k and l are kernels, $C^{k,l}$ is the cross-covariance operator in the Reproducing Kernel Hilbert Spaces (RKHS) of k and l, $||\cdot||_{\text{HS}}$ is the Hilbert-Schmidt norm [7, 8]. If we use radial basis function (RBF) kernels for k and l, HSIC is zero if and only if two random variables are independent.

Since we only have the finite number of samples drawn from the distributions, we need a finite sample estimator of HSIC. Following Bahng *et al*. [2], we employ an unbiased estimator of HSIC, $\text{HSIC}^{k,l}_1(Z_c,Z_s)$ [17] with m samples. Formally, $\text{HSIC}^{k,l}_1(Z_c,Z_s)$ is defined as:

$$
\begin{aligned}
\text{HSIC}^{k,l}_1(Z_c,Z_s) = \frac{1}{m(m-3)}\Bigg[&\text{tr}(\widetilde{Z}_c\widetilde{Z}_s^T) + \\
&\frac{\mathbf{1}^T\widetilde{Z}_c\mathbf{1}\mathbf{1}^T\widetilde{Z}_s^T\mathbf{1}}{(m-1)(m-2)} - \frac{2}{m-2}\mathbf{1}^T\widetilde{Z}_c\widetilde{Z}_s^T\mathbf{1}\Bigg]
\end{aligned} \tag{B.2}
$$

where (i, j)-th element of a kernel matrix $\widetilde{Z}_c$ is defined as, $\widetilde{Z}_c(i,j) = (1-\delta_{ij})\,k(f_c^i, f_c^j)$, and the i-th feature in the mini-batch f_c^i, is assumed to be sampled from the Z_c, *i.e.*, $\{f_c^i\} \sim Z_c$. We similarly define $\widetilde{Z}_s(i,j) = (1-\delta_{ij})\,l(f_s^i, f_s^j)$.

In practice, we compute $\text{HSIC}^{k,l}_1(Z_c,Z_s)$ in a mini-batch, *i.e.*, m is the batch size. We use the RBF kernel with kernel radius 0.5, *i.e.*, $k(f_c^i,f_c^j) = \exp(-\frac{1}{2}\|f_c^i - f_c^j\|_2^2)$.

B.4. GAN objective details

We employ two conditional discriminators D_s and D_c which predict a style label y_s and a content label y_c, respectively. In practice, we employ a multitask discriminator D, and different projection embeddings for content labels and style labels, following the previous methods [15, 4, 16]. The hinge loss [20] is employed to high fidelity generation:

$$
\begin{aligned}
\mathcal{L}^D_{adv} = \ &\mathbb{E}_{(x,y_c,y_s)}\left[[1-D(x,y_s)]_+ + [1-D(x,y_c)]_+\right]\\
&+\mathbb{E}_{(\widetilde{x},y_c,y_s)}\left[[1-D(\widetilde{x},y_s)]_+ + [1-D(\widetilde{x},y_c)]_+\right]\\
\mathcal{L}^G_{adv} = &-\mathbb{E}_{(\widetilde{x},y_c,y_s)}\left[D(\widetilde{x},y_s) + D(\widetilde{x},y_c)\right],
\end{aligned} \tag{B.3}
$$

where $\widetilde{x}$ is the generated image by combining a content feature extracted from an image with content label y_c and a style feature extracted from an image with style label y_s.

The feature matching loss $\mathcal{L}_{fm}$ and the reconstruction loss $\mathcal{L}_{recon}$ are formulated as follows:

$$
\begin{aligned}
\mathcal{L}_{fm} &= \mathbb{E}_{(x,\widetilde{x})}\left[\sum_{l=1}^{L-1}\|D^l(x) - D^l(\widetilde{x})\|_1\right],\\
\mathcal{L}_{recon} &= \mathbb{E}_{(x,\widetilde{x})}\left[\|x-\widetilde{x}\|_1\right],
\end{aligned} \tag{B.4}
$$

where L is the number of layers in the discriminator D and D^l denotes the output of l-th layer of D.

B.5. Training details

We use Adam [12] optimizer to optimize the MX-Font. The learning rate is set to 0.001 for the discriminator and 0.0002 for the remaining modules. The mini-batch is constructed with the target glyph, style glyphs, and content glyph during training. Specifically, we first pick the target glyph randomly. Then, we randomly select n style glyphs with the same style as the target glyph, and n content glyphs with the same character as the target glyph for each target glyph. Here, the target glyph is excluded from the style and content glyphs selection. We set n to 3 during training. We set the number of heads k to 6 and train the model for 650k iteration with the full objective functions for the Chinese glyph generation. For the Korean, we set the number of heads k to 3 and train the model for 200k iteration with the all objective functions except $\mathcal{L}_{\text{indp exp},i}$. We do not employ the $\mathcal{L}_{\text{indp exp},i}$ during training for the Korean glyph generation, due to the special characteristic of the Korean script; always decomposed to fixed number of components, *e.g.*, 3.

(a) User study example (Chinese generation)

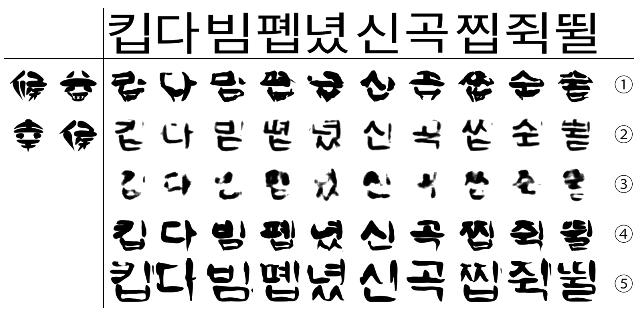

(b) User study example (Korean generation)

Figure C.1. **User study examples.** The example images that we provide to the candidates are shown. Each image includes the reference images, source images, and the generated images.

C. Evaluation details

C.1. Classifiers

Three classifiers are trained for the training; the style classifier, the Chinese character classifier, and the Korean character classifier. The style classifier and the Chinese character classifier are trained with the same Chinese dataset, including 209 Chinese fonts and 6428 Chinese characters per font. Besides, we used the Korean dataset that DM-Font [4] provides to train the Korean character classifier. The classifiers have ResNet-50 [9] structure. We optimize the classifiers using AdamP optimizer [10] with learning rate 0.0002 for 20 epochs. During training, the CutMix augmentation [19] is adopted and the mini-batch size is set to 64.

C.2. LF-Font modification

Since LF-Font [16] cannot handle the unseen components in the test time due to its component-conditioned structure, we modify its structure to enable the cross-lingual font generation. We loose the component-condition of LF-Font in the test time only, by skipping the component-condition block when the unseen component is given. Note that, we use original LF-Font structure for the training to reproduce its original performance.

	CN → CN			CN → KR		
FIDs	S	C	H	S	C	H
EMD	145.5	51.1	79.7	220.3	113.8	150.0
AGIS-Net	91.0	10.8	19.2	235.5	106.5	146.5
FUNIT	50.6	11.8	19.2	486.4	107.4	176.0
LF-Font	**43.5**	**9.0**	**14.8**	187.8	123.4	148.7
MX-Font	50.5	13.9	21.8	**113.2**	**78.1**	**84.1**

Table C.1. We provide style-aware (S), content-aware(C) FIDs measured by the style and content classifiers. The harmonic mean (H) of the style-aware and the content-aware FIDs values are identical to the values reported in the main table.

C.3. User study examples

We show the sample images used for the user study in Figure C.1. Five methods, including EMD [21], AGIS-Net [6], FUNIT [15], LF-Font [16], and MX-Font are randomly displayed to users for every query.

C.4. FID

We measure the style-aware and content-aware Frechét inception distance (FID) [11] between generated images and rendered images using the style and content classifier. For the Chinese glyphs, the style-aware and content-aware FIDs are measured with the generated glyphs and the corresponding ground truth glyphs. Since the ground truth glyphs of cross-lingual generation do not exist, the style-aware FID is measured the generated glyphs and all the available rendered glyphs having the same style with the generated images. The content-ware FID is measured similar to the style-aware FID. The style-aware (S) and the content-aware (C) FID values and their harmonic mean (H) are reported in Table C.1. Despite that MX-Font shows the slight degradation in FID for Chinese font generation, these results are not consistent with the user study and qualitative evaluation. For quantifying the image quality, we tend to trust the user study more because it better reveals the user's preference.

References

[1] Faez Ahmed, John P Dickerson, and Mark Fuge. Diverse weighted bipartite b-matching. *arXiv preprint arXiv:1702.07134*, 2017. 1

[2] Hyojin Bahng, Sanghyuk Chun, Sangdoo Yun, Jaegul Choo, and Seong Joon Oh. Learning de-biased representations with biased representations. In *ICML*, 2020. 3

[3] Yue Cao, Jiarui Xu, Stephen Lin, Fangyun Wei, and Han Hu. GCNet: Non-local networks meet squeeze-excitation networks and beyond. In *IEEE International Conference on Computer Vision Workshops*, 2019. 1

[4] Junbum Cha, Sanghyuk Chun, Gayoung Lee, Bado Lee, Seonghyeon Kim, and Hwalsuk Lee. Few-shot compositional font generation with dual memory. In *Eur. Conf. Comput. Vis.*, 2020. 3, 4

[5] Cheng Chen, Lan Zheng, Venkatesh Srinivasan, Alex Thomo, Kui Wu, and Anthony Sukow. Conflict-aware weighted bipartite b-matching and its application to e-commerce. *IEEE Transactions on Knowledge and Data Engineering*, 28(6):1475–1488, 2016. 1

[6] Yue Gao, Yuan Guo, Zhouhui Lian, Yingmin Tang, and Jianguo Xiao. Artistic glyph image synthesis via one-stage few-shot learning. *ACM Trans. Graph.*, 2019. 4

[7] Arthur Gretton, Olivier Bousquet, Alex Smola, and Bernhard Schölkopf. Measuring statistical dependence with hilbert-schmidt norms. In *International conference on algorithmic learning theory*, pages 63–77. Springer, 2005. 3

[8] Arthur Gretton, Kenji Fukumizu, Choon H Teo, Le Song, Bernhard Schölkopf, and Alex J Smola. A kernel statistical test of independence. In *Advances in neural information processing systems*, pages 585–592, 2008. 3

[9] Kaiming He, Xiangyu Zhang, Shaoqing Ren, and Jian Sun. Deep residual learning for image recognition. In *IEEE Conf. Comput. Vis. Pattern Recog.*, 2016. 4

[10] Byeongho Heo, Sanghyuk Chun, Seong Joon Oh, Dongyoon Han, Sangdoo Yun, Gyuwan Kim, Youngjung Uh, and Jung-Woo Ha. Adamp: Slowing down the slowdown for momentum optimizers on scale-invariant weights. In *Int. Conf. Learn. Represent.*, 2021. 4

[11] Martin Heusel, Hubert Ramsauer, Thomas Unterthiner, Bernhard Nessler, and Sepp Hochreiter. GANs trained by a two time-scale update rule converge to a local nash equilibrium. In *Advances in Neural Information Processing Systems*, 2017. 4

[12] Diederick P Kingma and Jimmy Ba. Adam: A method for stochastic optimization. In *ICLR*, 2015. 3

[13] Peter Kleinschmidt and Heinz Schannath. A strongly polynomial algorithm for the transportation problem. *Mathematical Programming*, 68(1):1–13, 1995. 1

[14] Harold W Kuhn. The hungarian method for the assignment problem. *Naval research logistics quarterly*, 2(1-2):83–97, 1955. 1

[15] Ming-Yu Liu, Xun Huang, Arun Mallya, Tero Karras, Timo Aila, Jaakko Lehtinen, and Jan Kautz. Few-shot unsupervised image-to-image translation. In *Int. Conf. Comput. Vis.*, 2019. 3, 4

[16] Song Park, Sanghyuk Chun, Junbum Cha, Bado Lee, and Hyunjung Shim. Few-shot font generation with localized style representations and factorization. In *AAAI*, 2021. 3, 4

[17] Le Song, Alex Smola, Arthur Gretton, Justin Bedo, and Karsten Borgwardt. Feature selection via dependence maximization. *Journal of Machine Learning Research*, 13(May):1393–1434, 2012. 3

[18] Sanghyun Woo, Jongchan Park, Joon-Young Lee, and In So Kweon. Cbam: Convolutional block attention module. In *ECCV*, 2018. 1

[19] Sangdoo Yun, Dongyoon Han, Seong Joon Oh, Sanghyuk Chun, Junsuk Choe, and Youngjoon Yoo. Cutmix: Regularization strategy to train strong classifiers with localizable features. In *Int. Conf. Comput. Vis.*, 2019. 4

[20] Han Zhang, Ian Goodfellow, Dimitris Metaxas, and Augustus Odena. Self-attention generative adversarial networks. In *ICML*, 2019. 3

[21] Yexun Zhang, Ya Zhang, and Wenbin Cai. Separating style and content for generalized style transfer. In *IEEE Conf. Comput. Vis. Pattern Recog.*, 2018. 4